Deficient binocular combination reveals mechanisms of anisometropic amblyopia: Signal attenuation and interocular inhibition

Chang-Bing Huang Laboratory of Brain Processes (LOBES), Department of Psychology, University of Southern California, Los Angeles, CA, USA

Jiawei Zhou School of Life Sciences, USTC, Hefei, Anhui, P.R. China

Zhong-Lin Lu Laboratory of Brain Processes (LOBES), Department of Psychology, University of Southern California, Los Angeles, CA, USA

Yifeng Zhou School of Life Sciences, USTC, Hefei, Anhui, P.R. China

Amblyopia is a developmental disorder that results in deficits of monocular and binocular vision. It is presently unclear whether these deficits result from attenuation of signals in the amblyopic eye, inhibition by signals in the fellow eye, or both. In this study, we characterize mechanisms underlying anisometropic amblyopia using a binocular phase and contrast combination paradigm and a contrast gain control model. Subjects dichoptically viewed two slightly different images and reported the perceived contrast and phase of the resulting cyclopean percept. We found that the properties of binocular combination were abnormal in many aspects in amblyopic vision. The observed abnormalities can be explained by a combination of (1) attenuated monocular signal in the amblyopic eye, (2) stronger interocular contrast gain control from the fellow eye to the signal in the amblyopic eye (direct interocular inhibition), and (3) stronger interocular contrast gain control from the fellow eye to the contrast gain control signal from the amblyopic eye (indirect interocular inhibition). We conclude that anisometropic amblyopia led to both monocular and interocular deficits. A complete understanding of the mechanisms underlying amblyopia requires studies of both monocular deficits and binocular interactions.

Keywords: low vision, binocular vision, contrast gain, computational modeling, visual development

Citation: Huang, C.-B., Zhou, J., Lu, Z.-L., & Zhou, Y. (2011). Deficient binocular combination reveals mechanisms of anisometropic amblyopia: Signal attenuation and interocular inhibition. *Journal of Vision, 11*(6):4, 1–17, http://www.journalofvision.org/content/11/6/4, doi:10.1167/11.6.4.

Introduction

Amblyopia, defined as degradation of vision in one eye without known optical or retinal causes, is a developmental disorder caused by early abnormal visual experiences, specifically a lack of registration between the images in the two eyes, most commonly due to uncorrected strabismus, anisometropia, or cataract-induced form deprivation. At a 2–4% prevalence rate (Ciuffreda, Levi, & Selenow, 1991), it leads to deficient visual acuity (Pugh, 1954), contrast sensitivity (Bradley & Freeman, 1981), grating acuity (Ciuffreda et al., 1991), contour integration (Hess & Demanins, 1998), global motion perception (Simmers, Ledgeway, Hess, & McGraw, 2003), spatial lateral interaction (Bonneh, Sagi, & Polat, 2007), and visual counting (Sharma, Levi, & Klein, 2000). Although many theories on amblyopia have focused on monocular deficits in the visual pathway associated with the amblyopic eye, such as signal attenuation (Baker, Meese, & Hess, 2008), under-sampling (Levi & Klein, 1986), topological jittering (Hess, Wang, Demanins, Wilkinson, & Wilson, 1999), reduced synchronization (Roelfsema, Konig, Engel, Sireteanu, & Singer, 1994), elevated internal noise (Baker et al., 2008; Huang, Tao, Zhou, & Lu, 2007; Levi & Klein, 2003; Xu, Lu, Qiu, & Zhou, 2006), and suboptimal perceptual template (Levi & Klein, 2003; Xu et al., 2006), the functional imbalance between the two eyes during abnormal development may lead to permanent changes to the cortical circuitry that affects not only the visual pathway associated with the amblyopic eye but also the pathway associated with the fellow eye and interactions between the two eyes (Harrad & Hess, 1992; Harwerth & Levi, 1983; Mitchell, Kind, Sengpiel, & Murphy, 2003; Smith & Trachtenberg, 2007). Indeed, results from physiological studies suggest that amblyopia is a cortical disorder with both striate and extrastriate origins (Kiorpes & McKee, 1999; but see Hess, Thompson, Gole, & Mullen, 2009). Furthermore, many

doi: 10.1167/11.6.4 Received October 26, 2010; published May 5, 2011 ISSN 1534-7362

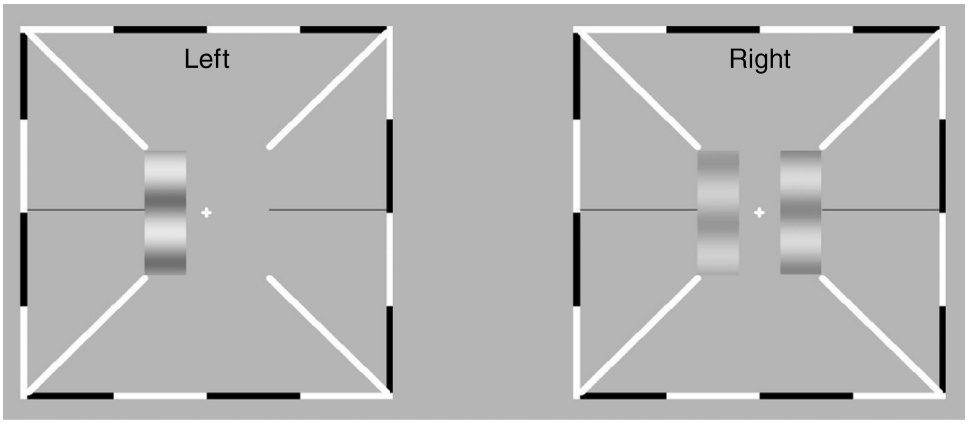

Figure 1. Stimulus display. The stimuli were delivered to the left and right eyes using a stereoscope. The two test gratings, on the left in the two eyes' views, differing in contrast and phase, are combined via a stereoscope. Observers adjusted the contrast and phase of the monocular probe grating to match those of the cyclopean images.

psychophysical studies have documented binocular and/or interocular deficits in amblyopia (Mitchell, Reardon, & Muir, 1975; Wood, Fox, & Stephenson, 1978), and several have concluded that the degree of binocularity is a good predictor of the abnormalities in monocular tasks (Kiorpes & McKee, 1999; McKee, Levi, & Movshon, 2003). A complete understanding of the mechanisms underlying amblyopia requires studies of both monocular deficits and binocular interactions.

In this study, we characterize both monocular and binocular deficits in anisometropic amblyopia using a binocular phase and contrast combination paradigm and a contrast gain control model that explains the appearance of cyclopean percepts from binocular combination of suprathreshold monocular images (Huang, Zhou, Zhou, & Lu, 2010). In this paradigm (Figure 1), a stereoscope is used to present two horizontal sine-wave gratings (test gratings), with the same spatial frequency but different contrasts and phases, to the two eyes; the cyclopean image that results on the left of fixation is compared to a probe grating presented monocularly to the right of fixation in one eye. The cyclopean percept is measured by requiring observers to adjust the phase and contrast of the probe grating to match those of the cyclopean percept. The perceived phase and contrast that result from binocular combination are measured as a function of the contrast in the amblyopic eye (base contrast), the ratio of the grating contrasts in the fellow and amblyopic eyes, the phase difference between the two test gratings, the eye in which the probe grating resides, and the dichoptic configuration (+ and − phase shifts in the amblyopic and fellow eyes and vice versa).

In a previous study (Huang et al., 2010), we successfully modeled the complex data pattern of binocular combinations of phase and contrast observed in normal observers using a multi-channel model (MCM) of contrast gain control by elaborating a contrast gain control theory of binocular phase combination (Ding & Sperling, 2006, 2007). In the MCM (Figures 2A–2E; Appendix A), signals in the two eyes first pass through interocular contrast gain control, in which each eye exerts gain control not only on the other eye's visual signal (path A2 and its counterpart in Figure 2A) but also on the incoming gain control signal from the other eye (path A3 and its counterpart in Figure 2A)—with both effects in proportion to an eye's own signal contrast energy. The perceived phase and contrast of the cyclopean percept are computed in separate pathways.

Here, we elaborate this model to develop signatures of three potential mechanisms of amblyopia (Figures 2F–2K; Appendix B): a monocular mechanism that attenuates signals in the amblyopic eye (Figures 2F and 2G), an interocular mechanism in which the fellow eye exerts stronger contrast gain control on signals in the amblyopic eye (direct interocular inhibition; Figures 2H and 2I), and another interocular mechanism in which the fellow eye exerts stronger contrast gain control on the gain control signals from the amblyopic eye (indirect interocular inhibition; Figures 2J and 2K). As shown in Figure 2, the three mechanisms have different signature performance patterns when perceived phase and particularly perceived contrast are plotted against the interocular contrast ratio of the test stimuli. Signal attenuation in the amblyopic eye would greatly reduce the strength of the amblyopic eye in both binocular phase and contrast combination; increasing the base contrast in the amblyopic eye would not change the effective contrast ratio in binocular phase combination; placing the probe in the fellow eye (solid curves) and the amblyopic eye (dashed curves) would cause a vertical shift in the perceived contrast versus contrast ratio curves in binocular contrast combination. Direct interocular inhibition would greatly reduce the strength of the internal representation of the grating in the amblyopic eye; increasing the base contrast in the amblyopic eye would increase the effective contrast ratio in binocular phase combination;

placing the probe in the fellow eye and the amblyopic eye would generate the same results in binocular contrast combination. Indirect interocular inhibition would greatly reduce the strength of the internal representation of the grating in the amblyopic eye; increasing the base contrast in the amblyopic eye would decrease the equivalent contrast ratio in binocular phase combination; placing the probe in the fellow eye and the amblyopic eye would generate the same results in binocular contrast combination. Measuring both perceived phase and contrast in binocular combination with different base contrast levels and with probe gratings in both the fellow and amblyopic eyes would allow us to distinguish the contributions from each potential mechanism of amblyopia. Our previous study, based on measures of perceived phase of the cyclopean images, was not successful in separating the three different mechanisms (Huang, Zhou, Lu, Feng, & Zhou, 2009).

Four naturally occurring anisometropic amblyopes (Table 1), with normal visual acuity (20/20–20/14) in the fellow eye and acuity ranging between 20/200 and 20/60 in the amblyopic eye, adjusted the phase and contrast of the probe grating to match those of the cyclopean percept. The perceived phase and contrast were measured in a total of 216 (3 base contrasts × 6 interocular contrast

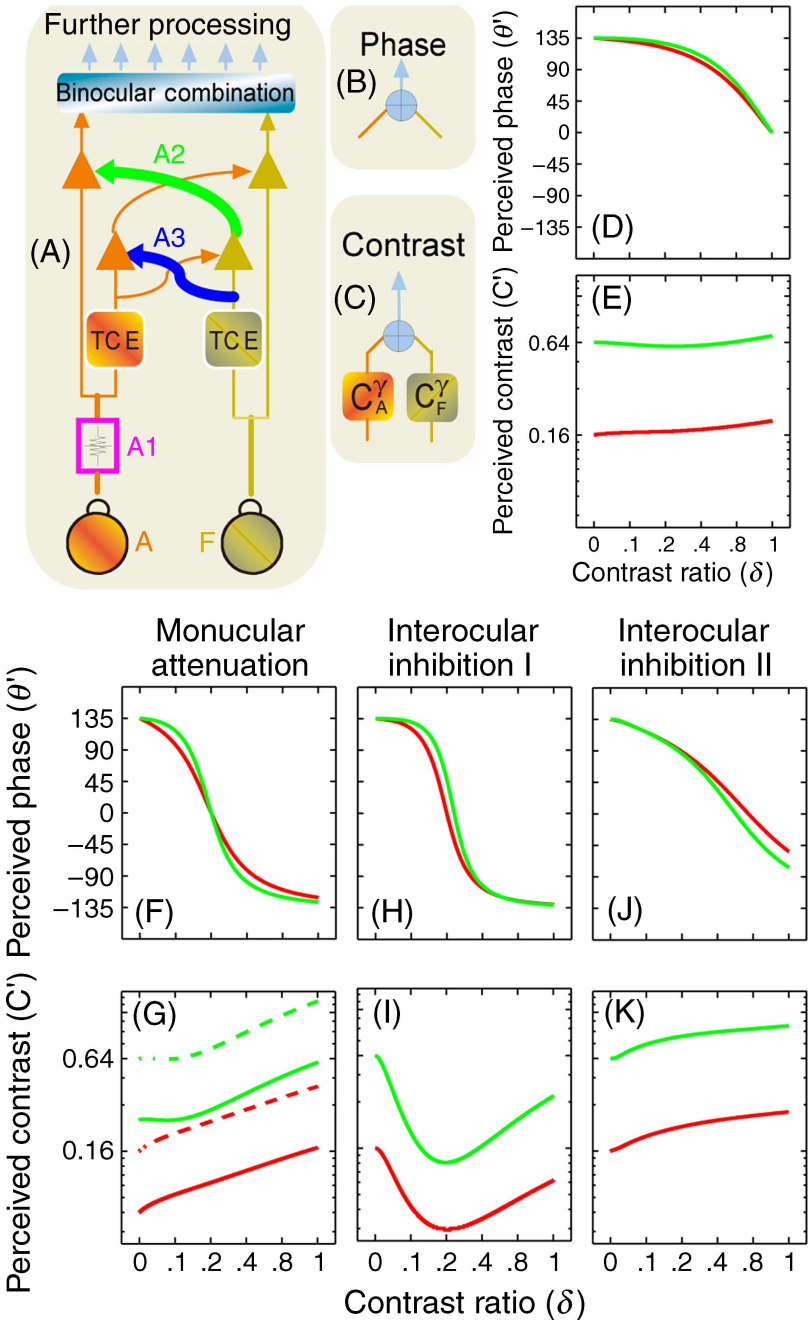

			AE		FE	
	Sex	Age	Refraction	VA*	Refraction	VA*
N1	M	20	+1.25DS/0.50DC × 90	1.8	−1.50DS/−0.50DC × 180	0.8
N2	M	21	+2.50DS/1.00DC × 60	2.5	−3.00DS/0.50DC × 15	1.0
N3	F	23	+2.50DS	2.0	Plano	0.7
N4	M	20	+2.75DS	2.0	Plano	0.7

Table 1. Characteristics of the four anisometropic amblyopes. *Notes*: Letter acuity was measured with the Tumbling E chart and expressed in minimum angle of resolution (MAR); AE, amblyopic eye; FE, fellow eye.

ratios × 3 phase differences × 2 probe eye conditions × 2 configurations) conditions. Mechanisms of amblyopia were identified by fitting the empirical data with MCMs.

Materials and methods

Observers

Four adult observers (20–23 years old), with naturally occurring anisometropia (Table 1) and naive to the purpose of the experiment, participated in the study with informed consents. Subjects wore their reflective corrections during the entire experiment (see Table 1). The research protocol was approved by the Ethics Committee of the University of Science and Technology of China.

Apparatus

All stimuli were generated by a PC computer running Matlab (MathWorks) with PsychToolBox 2.54 extensions (Brainard, 1997; Pelli, 1997) and presented on a Sony G220 Triniton monitor with a 1600 × 1200 resolution and a 75-Hz vertical refresh rate. A special circuit (http://lobes.usc.edu/videoswitcher.html) was used to combine two 8-bit output channels of the video card to yield 14-bit grayscale levels (Li, Lu, Xu, Jin, & Zhou, 2003) that was then scaled linearly using a psychophysical procedure (Li et al., 2003). A modified Helioth–Wheatstone stereoscope (Dudley, 1951; Wheatstone, 1838) was used to present the dichoptic images to the two eyes. The stereoscope and a chin rest were mounted on a table with a 105-cm total optical path.

Stimuli

Stimuli were three horizontal sine-wave gratings, each subtending 0.67 × 2 deg^2 (Figure 1). The luminance profiles of the two test gratings in the left visual field of the amblyopic and fellow eyes are given by the following equations:

$$\mathrm{Lum_L}(y) = L_0\left[1 - C_0\cos\left(2\pi f y \pm \frac{\theta}{2}\right)\right], \quad (1)$$

$$\mathrm{Lum_R}(y) = L_0\left[1 - \delta C_0\cos\left(2\pi f y \mp \frac{\theta}{2}\right)\right], \quad (2)$$

Figure 2. Signature performance patterns of the three potential mechanisms of amblyopia. (A–C) The multi-channel contrast gain control model (MCM; Huang et al., 2010) of binocular combination. (A) Signals in the two eyes first go through double contrast gain control, in which each eye exerts gain control not only on the other eye's visual signal (path A2 and its counterpart) but also on the incoming gain control signal from the other eye (path A3 and its counterpart)—both effects in proportion to an eye's own signal contrast energy. Computations of (B) phase and (C) contrast combination were then carried out separately. (D, E) Signature performance patterns of cyclopean phase and contrast perception in normal subjects. Red curves: base contrast = 0.16; green curves: base contrast = 0.64. (F, G) Signal attenuation in the amblyopic eye (A1 in (A)) would greatly reduce the strength of the amblyopic eye in both binocular phase and contrast combination; increasing the base contrast in the amblyopic eye would not change the effective contrast ratio in binocular phase combination; placing the probe in the fellow eye (solid curves) and the amblyopic eye (dashed curves) would cause a vertical shift in the perceived contrast versus contrast ratio curves in binocular contrast combination. (H, I) Direct interocular inhibition: stronger contrast gain control of the fellow eye on the signal in the amblyopic eye (A2) would greatly reduce the strength of the internal representation of the grating in the amblyopic eye; increasing the base contrast in the amblyopic eye would increase the effective contrast ratio in binocular phase combination; placing the probe in the fellow eye and the amblyopic eye would generate the same results in binocular contrast combination (dashed and solid curves). (J, K) Indirect interocular inhibition: stronger contrast gain control of the fellow eye on the gain control signal from the amblyopic eye (A3) would greatly reduce the strength of the internal representation of the grating in the amblyopic eye; increasing the base contrast in the amblyopic eye would decrease the equivalent contrast ratio in binocular phase combination; placing the probe in the fellow eye and the amblyopic eye would generate the same results in binocular contrast combination (dashed and solid curves).

where $L_0 = 31.2$ cd/m^2 is the background luminance, $f = 1$ c/deg is the spatial frequency of the gratings, C_0 is the base contrast, and δ is the interocular contrast ratio. The two gratings are phase-shifted in opposite directions by $\frac{\theta}{2}$, with a total phase difference of θ. All gratings were displayed for exactly 2 cycles. The two monocular test sine-wave gratings were viewed through the stereoscope to generate a single cyclopean sine-wave grating. Three base contrasts ($C_0 \in \{0.16, 0.32, 0.64\}$), six interocular contrast ratios ($\delta \in \{0, 0.1, 0.2, 0.4, 0.8, 1.0\}$), and three phase differences ($\theta \in \{45°, 90°, 135°\}$) were tested.

The probe grating, presented in either in the amblyopic or the fellow eye, was defined by

$$\mathrm{Lum_P}(y) = L_0[1 - C_\mathrm{P} \cos(2\pi f y + \theta_\mathrm{P})], \quad (3)$$

where $f = 1$ c/deg is the same as that of the test gratings, and both the contrast and phase, C_P and θ_P, of the probe grating were adjusted by the observer to match those of the cyclopean image on the left side of the display.

Procedure

Each trial began with a fixation display consisting of a fixation cross (0.11×0.11 deg^2) and a high-contrast frame (width: 0.11 deg; length: 6 deg) with diagonal bars (width: 0.11 deg; length: 2.33 deg) in each eye (Figure 1). The high-contrast frames remained on the screen during the entire experiment to assist observers to fuse images from the two eyes. After achieving correct vergence, the observer pressed the space bar on the computer keyboard to initiate the presentation of the three sine-wave gratings: two test gratings on the left and a probe grating on the right, with the initial contrast and phase of the probe grating set randomly. Observers were required to adjust the contrast and phase of the probe grating to match those of the cyclopean image on the left. They were free to select which dimension to adjust first and to go back and forth between them and pressed the "Enter" key twice to report the results after they were satisfied with the match in both dimensions. A typical trial lasted about 10 s.

Design

We measured the perceived phase and contrast of the cyclopean image as a function of the base contrast level, the contrast ratio between the two eyes, the phase difference between the two test sine-wave gratings, and stimulus configuration. Two stimulus configurations were used to cancel potential positional biases (Ding & Sperling, 2006; Huang et al., 2009): (a) amblyopic eye phase shift = $\theta/2$, fellow eye phase shift = $-\theta/2$ and (b) amblyopic eye phase shift = $-\theta/2$, fellow eye phase shift = $\theta/2$. Following Ding and Sperling (2006), we scored the perceived phase of the cyclopean sine wave as the difference between the measurements from the two configurations. There were, therefore, a total of 216 (3 base contrasts $\times$ 6 interocular ratios $\times$ 3 phase differences $\times$ 2 probe eyes $\times$ 2 configurations) conditions.

Each experimental session consisted of one measurement in all experimental conditions, lasting 40 to 90 min. The measurements were repeated at least 8 times on separate days. Voluntary breaks were allowed. Practice trials were provided prior to data collection.

Data analysis

Within-subject Analysis of Variance (ANOVA) was used to test whether the perceived contrast/phase is dependent on the probe eye condition, the phase shift, the base contrast level, the interocular contrast ratio, and their interactions. We also evaluated the correlation between the equivalent contrast ratio (the interocular contrast ratio at which the two eyes contribute equally) in binocular phase combination and visual acuity and contrast sensitivity ratios using SPSS.

All the model-fitting procedures were implemented in Matlab using a non-linear least-square method that minimized $\sum(y_i^{\mathrm{predicted}} - y_i^{\mathrm{measured}})^2$, where y_i^{measured} and $y_i^{\mathrm{predicted}}$ denote measured values and the corresponding model predictions, respectively. The goodness of fit was evaluated by the r^2 statistic for phase and contrast separately:

$$r^2 = 1.0 - \frac{\sum(y_i^{\mathrm{predicted}} - y_i^{\mathrm{measured}})^2}{\sum[y_i^{\mathrm{measured}} - \mathrm{mean}(y_i^{\mathrm{measured}})]^2}. \quad (4)$$

An F-test for nested models was used to statistically compare the models based on the average r^2s of phase and contrast. For two nested models with k_{full} and k_{reduced} parameters, the F statistic is defined as

$$F(df_1, df_2) = \frac{(r^2_{\mathrm{full}} - r^2_{\mathrm{reduced}})/df_1}{(1 - r^2_{\mathrm{full}})/df_2}, \quad (5)$$

where $df_1 = k_{\mathrm{full}} - k_{\mathrm{reduced}}$, and $df_2 = N - k_{\mathrm{full}}$; N is the number of data points.

Results

Perceived phase of the cyclopean gratings

The perceived phase θ' of the cyclopean percept is plotted as a function of the contrast ratio between the test gratings in the two eyes for individual subjects in

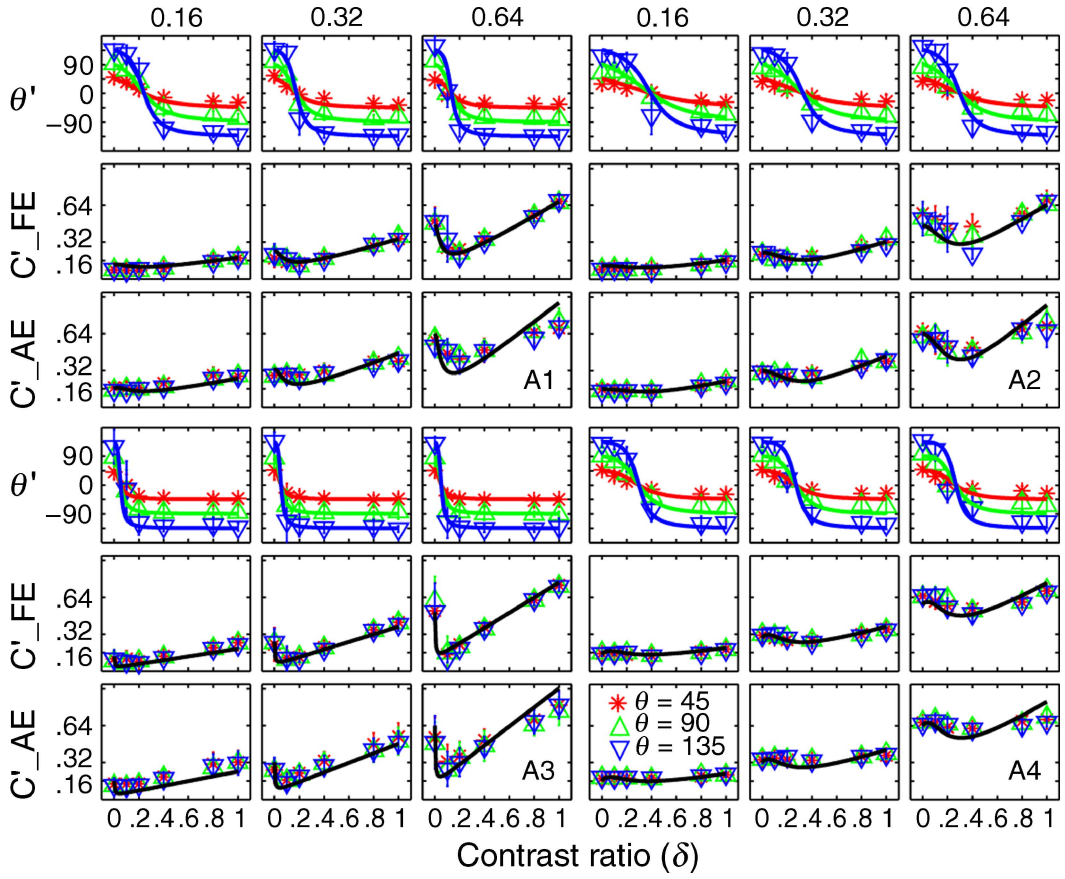

Figure 3. Perceived contrast and phase of the cyclopean gratings for four individual subjects. For each observer, data from the three base contrast conditions are shown in three columns. Within each column, the upper row shows the perceived phase (in degrees), the middle row shows the perceived contrast when the probe grating is in the fellow eye, and the lower row shows the perceived contrast when the probe grating is in the amblyopic eye. Different colors denote different phase shift conditions: red asterisk for 45 deg, green upward-pointing triangle for 90 deg, and blue downward-pointing triangle for 135 deg. Error bars represent standard deviations.

Figure 3, and for the average subject in Figure 4A, with data from the three base contrast conditions presented in separate columns. Within each column, the upper row shows the perceived phase (in degrees), the middle row shows the perceived contrast when the probe grating is in the fellow eye, and the lower row shows the perceived contrast when the probe grating is in the amblyopic eye. Different colored lines and symbols denote different phase shift conditions. The perceived phase of the cyclopean image depended on the contrast ratio of the sine-wave gratings in the two eyes ($F(5,15) = 52.44$, $P < 0.001$) but not on the eye of the probe ($F(1,3) = 0.14$, $P > 0.50$) or base contrast ($F(2,6) = 0.05$, $P > 0.90$). Data from the two probe eye conditions were pooled in Figure 3 and in subsequent analyses.

As the interocular contrast ratio increased from 0 (when the test consisted of a single grating in the amblyopic eye) to 1.0 (when the test consisted of gratings with equal contrast in both eyes), the perceived phase of the cyclopean grating monotonically decreased from approximately +45, +90, and +135 deg to −45, −90, and −135 deg in the three phase shift conditions, respectively (Figures 3 and 4A). Because the gratings in the two eyes were always phase-shifted with equal magnitude but in opposite directions, the perceived phase of the cyclopean image should be 0 deg when the internal representations of the two gratings exhibit equal strength in binocular combination; the shift from positive to negative phase values signified the transition from greater internal signal strength in the amblyopic eye to greater internal signal strength in the fellow eye. The zero-crossing point of the phase versus contrast ratio curve defines the effective contrast ratio of the amblyopic eye relative to the fellow eye in binocular phase combination. Averaged over base contrast levels and phase differences, the effective contrast ratio of the amblyopic eye was 0.19 ± 0.09 (mean ± *SD*), 0.31 ± 0.06, 0.07 ± 0.02, and 0.26 ± 0.04 for the four subjects, respectively. The amblyopic eye is thus much less effective in binocular phase combination (Ding, Klein, & Levi, 2009; Huang et al., 2009), consistent with all three potential mechanisms of amblyopia (Figures 2F, 2H, and 2J).

The effective contrast ratio decreased significantly as the base contrast increased in binocular phase combination in amblyopia ($F(2,8) = 10.53$, $P < 0.01$). Averaged across subjects, the effective contrast ratio is 0.26 ± 0.11 (mean ± *SD*),

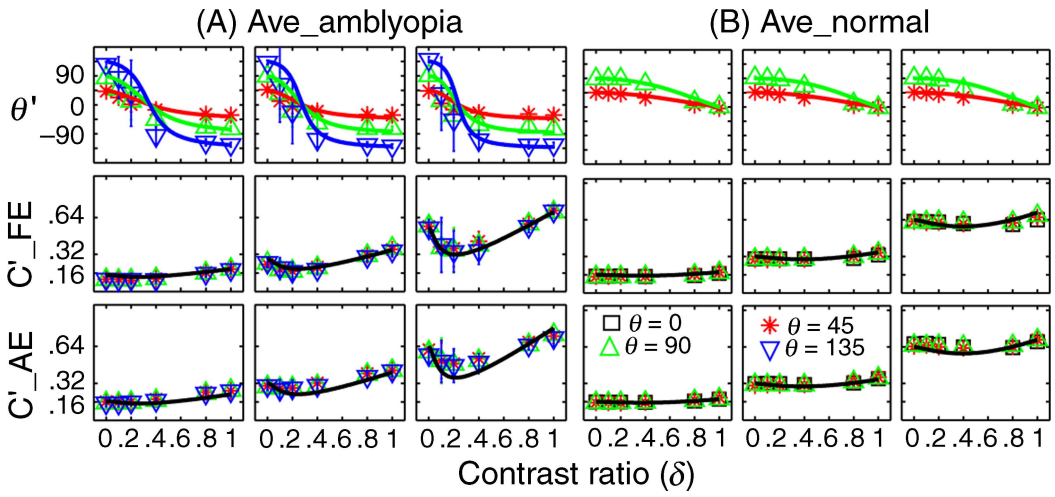

Figure 4. Average perceived contrast and phase of the cyclopean gratings for the (A) amblyopic subjects in this study and (B) normal subjects in Huang et al. (2010). Data from the three base contrast conditions are shown in three columns. Within each column, the upper row shows the perceived phase (in degrees), the middle row shows the perceived contrast when the probe grating is in the fellow/right eye, and the lower row shows the perceived contrast when the probe grating is in the amblyopic/left eye. Different colors denote different phase shift conditions: black square for 0 deg, red asterisk for 45 deg, green upward-pointing triangle for 90 deg, and blue downward-pointing triangle for 135 deg. Error bars represent standard deviations.

0.19 ± 0.09, and 0.16 ± 0.09, in the three base contrast conditions. This is consistent with Ding et al. (2009). The pattern of results suggests contributions of indirect interocular inhibition, i.e., the fellow eye exerts stronger contrast gain control on the gain control signals from the amblyopic eye (Figure 2J).

To compare these results to those of the normal subjects, we replot in Figure 4B the average phase and contrast versus interocular contrast ratio curves of the four normal 22- to 28-year-old subjects in Huang et al. (2010). The same experimental procedure was used to investigate binocular phase and contrast combination in these normal subjects except that the measurements were performed in one in-phase condition and two out-of-phase conditions ($\theta \in \{0°, 45°, 90°\}$) for the perceived contrast and two out-of-phase conditions for the perceived phase ($\theta \in \{45°, 90°\}$). For the normal subjects, the zero-crossing point of the phase versus contrast ratio curve was almost 1.0 (Figure 4B), indicating that the two eyes are essentially equivalent in binocular phase combination (Ding & Sperling, 2006; Huang et al., 2010).

Perceived contrast of the cyclopean gratings

The perceived contrast of the cyclopean gratings, C', is plotted as a function of interocular contrast ratio, with data from the three base contrast and two probe eye conditions presented in separate panels in Figures 3 and 4A. The value of C' depended critically on interocular contrast ratio ($F(5,15) = 7.48$, $P < 0.001$). The strongly curved shape of the function relating perceived contrast versus contrast ratio suggests contributions of the direct interocular inhibition mechanism of amblyopia (Figure 2I), i.e., the fellow eye exerts stronger contrast gain control on the incoming signals from the amblyopic eye. Because the two dichoptic stimulus configurations yielded essentially identical estimates ($F(1,3) = 1.67$, $P > 0.25$), we pooled the data in the two dichoptic configurations in subsequent analyses.

Consistent with our observations on normal subjects (Huang et al., 2010), the perceived contrast of the cyclopean gratings did not significantly depend on the phase difference of the two test sine-wave gratings in any of the three base contrast conditions ($F(4,12) = 2.50$, $P > 0.10$). In Figures 5A and 5B, we replot the average perceived contrast (C') of the cyclopean images as functions of interocular phase difference (θ) for the amblyopic subjects in this study and the normal subjects in Huang et al. (2010). For both groups of subjects, all perceived contrast versus phase shift curves are essentially flat, although the perceived contrasts at the six interocular contrast ratio conditions are more scattered for subjects with amblyopia. Control experiments on normal subjects showed that the effect was not due to high spatial-frequency contaminations (Cormack, Stevenson, & Landers, 1997). In contrast, any phase-dependent binocular contrast combination model would predict a factor of 2.41 between the 45- and 135-deg phase shift conditions when the internal representations of the two monocular gratings are the same (Appendix A). This prediction is clearly not consistent with the data.

The average (across base contrast level, phase shift between monocular images, and subjects) normalized perceived contrast, defined as the perceived contrast divided by the base contrast in each condition, is plotted in

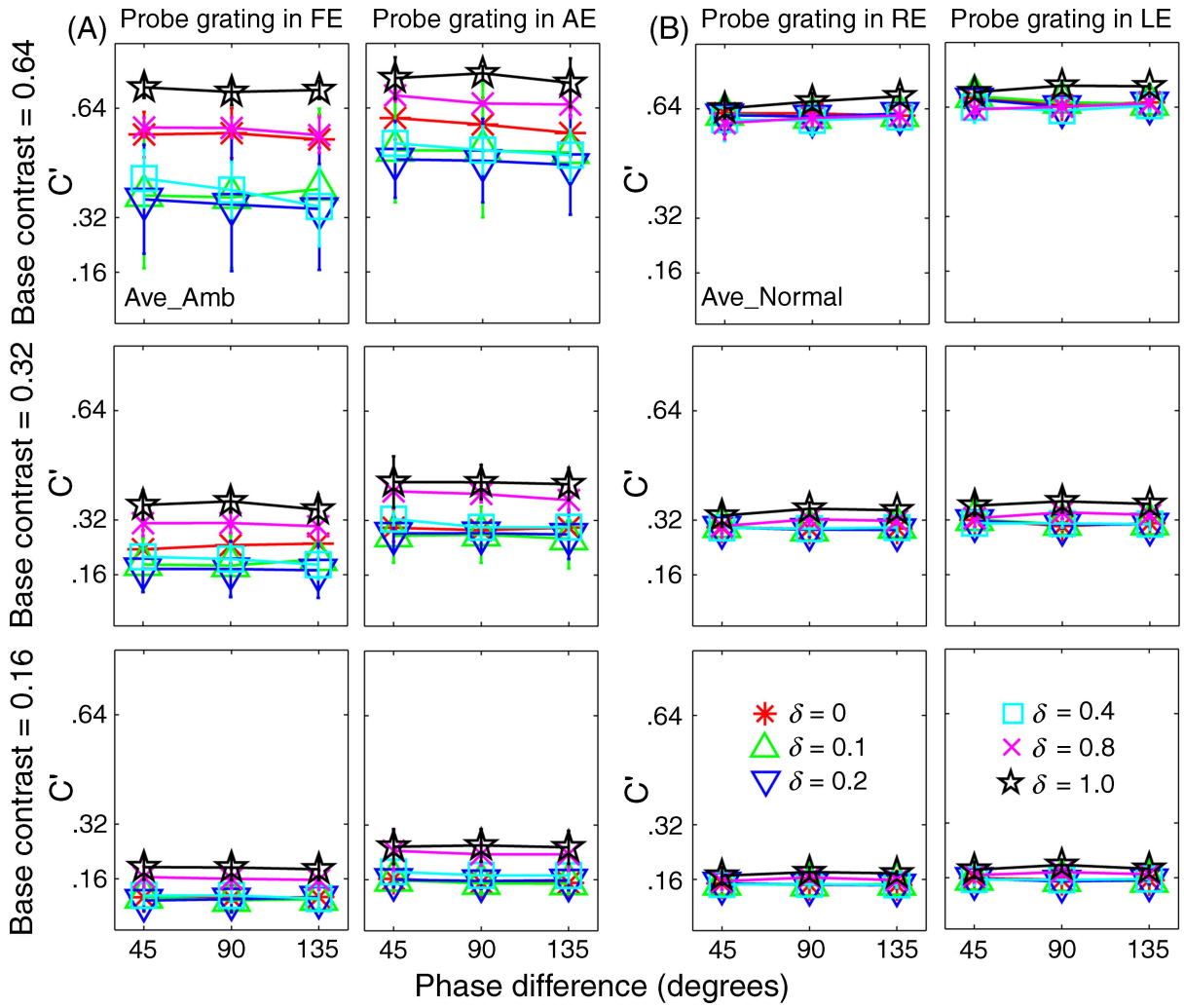

Figure 5. Average perceived contrast (C') of the cyclopean images versus interocular phase difference curves for the (A) amblyopic subjects in this study and (B) normal subjects in Huang et al. (2010). Red asterisks, green upward-pointing triangles, blue downward-pointing triangles, cyan squares, magenta crosses, and black five-pointed stars represent data from the six contrast ratio conditions (δ = 0, 0.1, 0.2, 0.4, 0.8, and 1.0).

Figure 6 as a function of interocular contrast ratio between the monocular images for both the amblyopic subjects in this study (Figure 6A) and the normal subjects in Huang et al. (2010; Figure 6B). For normal subjects, the normalized contrast is very close to 1.0 for contrast ratios up to 0.8 and goes to 1.15 when the contrast ratio is 1.0. As shown in Huang et al. (2010), a simple equation, $C' = (C_0^{6.17} + \delta^{6.17} C_0^{6.17})^{1/6.17}$, can be used to describe the perceived contrast as a function of the base contrast and the interocular contrast ratio between the two eyes. For subjects with amblyopia, on the other hand, the normalized perceived contrast versus interocular contrast ratio function is a U-shaped function. Its value decreases to 0.86 when the interocular contrast ratio is 0.2 and then increases to 1.48 when the interocular contrast ratio is 1.0, indicating strong non-linear interactions between the amblyopic and fellow eyes.

Each binocular combination condition provided two estimates of the perceived contrast, with the probe in either the amblyopic or the fellow eye (Figures 3 and 4A). The probe eye had a significant effect ($F(1,3) = 40.47$, $P < 0.01$), suggesting contributions of the monocular attenuation mechanism of amblyopia (Figure 2G). Because identical binocular stimuli were used in the two probe conditions, the ratio between the matched contrasts in the two probe eye conditions provides one measure of the relative efficiency of the two eyes. Averaged across all the experimental conditions, the ratio is 0.65 ± 0.16 (mean ± *SD*), 0.72 ± 0.12, 0.74 ± 0.16, and 0.86 ± 0.08 for the four subjects. This ratio, which can also be obtained by matching the contrast of two monocular sine waves presented at adjacent visual field locations in the amblyopic and fellow eyes, reflects the "monocular" strength of the two eyes when there is no interocular interaction in the corresponding

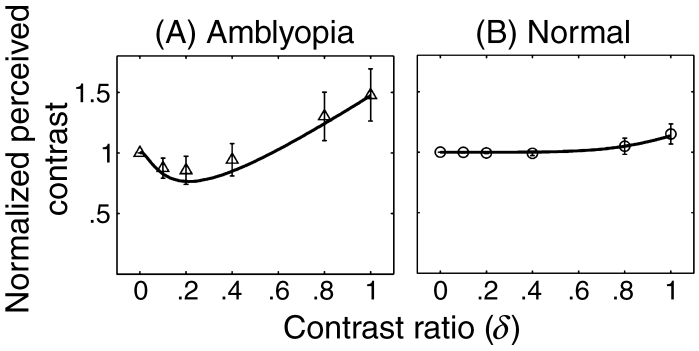

Figure 6. Normalized average perceived contrast versus interocular contrast ratio curves for the (A) amblyopic subjects in this study and (B) normal subjects in Huang et al. (2010). In (A), the solid curve represents the best fit of the model with signal attenuation and equal direct and indirect inhibition. In (B), the curve represents the best fit with the equation $C'/C_0 = (1 + \delta^{\upsilon})^{1/\upsilon}$ with υ = 6.17. The simple descriptive equation provided similar fits as the MCM model but facilitated the derivation of effective contrast ratio in amblyopia.

retinal locations. In comparison, for the three subjects with contrast sensitivity function (CSF) data obtained in another experiment, the contrast sensitivity ratio between the amblyopic and fellow eyes was 1.02, 0.98, and 0.79 at the 1.0 c/deg spatial frequency tested in binocular combination. In other words, deficits in monocular contrast sensitivity cannot account for the observed binocular combination deficits in anisometropic amblyopia, supporting the notion that monocular and binocular deficits represent two independent dimensions of spatial vision deficits in amblyopia (McKee et al., 2003).

To estimate the effective contrast ratio of the amblyopic eye in binocular contrast combination when signals are present in both eyes, we first computed how much contrast in the amblyopic eye would be needed, if the amblyopic eye were "normal," to obtain the observed contrast in each contrast ratio conditions. Data were first averaged across phase shift conditions. In each contrast ratio condition, the contrast in the amblyopic eye is C_0, the contrast in the fellow eye is δC_0, and the matched probe contrast in the fellow eye is C'. If the amblyopic eye were normal and were presented with a grating with a contrast of C_n, following the result from normal subjects (Figure 6B; Huang et al., 2010), the matched contrast in the fellow eye would be $C' = (C_n^{6.17} + \delta^{6.17} C_0^{6.17})^{1/6.17}$. Inverting the equation, we obtain $C_n = (C'^{6.17} - \delta^{6.17} C_0^{6.17})^{1/6.17}$. We defined $\frac{C_n}{C_0}$ as the effective contrast ratio of the amblyopic eye in binocular contrast combination.

As shown in Figure 7, the effective contrast of the amblyopic eye depended critically on the contrast ratio between the two monocular test gratings ($F(5,15) = 4.97$, $P < 0.01$) but not on base contrast ($F(2,6) = 1.18$, $P > 0.35$). As the contrast ratio between the images in the fellow eye and the amblyopic eye increases from 0 to 1.0, the effective contrast ratio first decreased from 0.76 ± 0.17 (mean ± *SD*) at $\delta = 0$, reaching its valley of 0.58 ± 0.23 at $\delta = 0.2$, and then increased to about 1.01 ± 0.21 at $\delta = 1.0$. The V-shaped function reflects asymmetric nonlinear interactions between the amblyopic and fellow eyes, suggesting contributions of interocular mechanisms of amblyopia.

Modeling

A model lattice consisting of all possible combinations of the three mechanisms (Figure 2), signal attenuation in the amblyopic eye (A1), direct interocular inhibition, i.e., stronger contrast gain control of the fellow eye on the signal in the amblyopic eye (A2), and indirect interocular inhibition, i.e., elevated contrast gain control of the fellow eye on the incoming gain control signal from the amblyopic eye (A3), were fit to all the empirical data. The most reduced model in the lattice is a model of the normal observer in which A1 = A2 = A3 = 1. The model with signal attenuation in the amblyopic eye (A1) and equal direct and

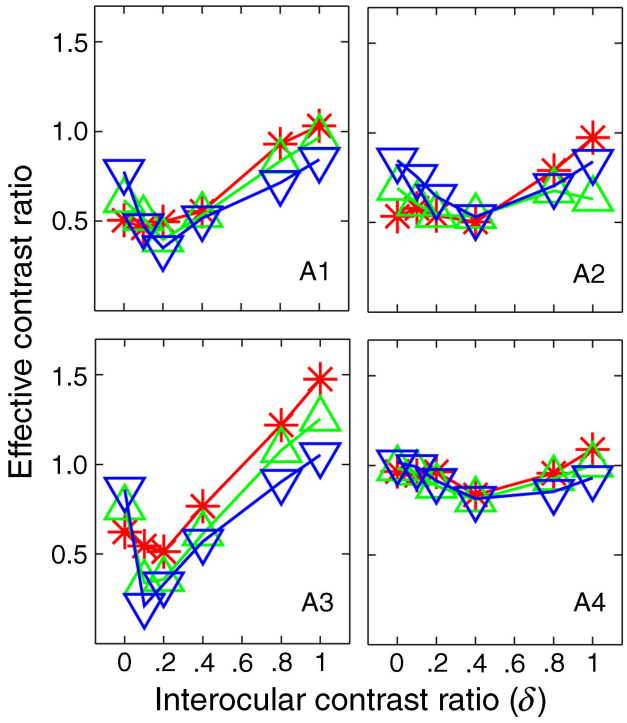

Figure 7. Effective contrast ratio as a function of interocular contrast ratio. Data were first averaged across phase shift conditions. In each contrast ratio condition, the contrast in the amblyopic eye is C_0, the contrast in the fellow eye is δC_0, and the matched contrast in the fellow eye is C'. If the amblyopic eye were "normal" and were presented with a grating with a contrast of C_n, following the result from normal subjects (Huang et al., 2010), the matched contrast in the fellow eye would be $C' = (C_n^{6.17} + \delta^{6.17} C_0^{6.17})^{1/6.17}$. Inverting the equation, we obtain $C_n = (C'^{6.17} - \delta^{6.17} C_0^{6.17})^{1/6.17}$. We defined $\frac{C_n}{C_0}$ as the effective contrast ratio of the amblyopic eye in binocular contrast combination.

	A1	A2 = A3	γ_1	γ_2	ρ	$r^2_{\_contrast}$	$r^2_{\_phase}$
N1	0.74	178.83	1.49	0.69	1.57	0.95	0.98
N2	0.78	9.84	1.25	0.79	15.19	0.97	0.97
N3	0.80	214.85	0.97	0.43	143.66	0.94	0.99
N4	0.90	46.54	2.13	0.53	92.34	0.98	0.96
AVE	0.86	31.45	1.35	0.78	3.04	0.99	0.99

Table 2. Parameters of the best fitted model.

indirect interocular inhibition (A2 = A3) explained 95%, 97%, 94%, 98%, and 99% variance of the contrast data and 98%, 97%, 99%, 96%, and 99% variance of the phase data for the four individual subjects and their average, respectively (Table 2). It provided statistically equivalent accounts as the full model with all six parameters free to vary, for both individual and average data, and its fits were superior to all its reduced parameter versions (e.g., the A1 model with A2 = A3 = 1, the A2 = A3 model with A1 = 1, the model with A1 = A2 = A3 = 1; all $p < 0.01$). The model with A1 and A2 = A3 is also superior to the original Ding–Sperling model that predicts phase-dependent contrast combination in all observers and their average for binocular contrast combination ($p < 0.01$). We conclude that signals in the amblyopic eye are attenuated in binocular combination, and the fellow eye exerts stronger contrast gain control on signal in the amblyopic eye and also on the contrast gain control signal from the amblyopic eye (both direct and indirect interocular inhibition).

Discussion

In this study, we developed a new theoretical framework to characterize both monocular and binocular deficits in anisometropic amblyopia based on the appearance of cyclopean percepts produced from binocular combination of suprathreshold monocular images. We found that (1) signals in the amblyopic eye were weighted much lower than signals in the fellow eye in binocular phase combination, (2) the effective contrast ratio decreased as the base contrast in the amblyopic eye increased in binocular phase combination, (3) binocular contrast combination was independent of the relative phase of the two monocular images, and (4) the effective contrast ratio of the amblyopic eye depended on the contrast ratio of the images in the two eyes in binocular contrast combination. The empirical pattern of results suggests contributions from all three potential mechanisms of amblyopia. Quantitative modeling found that signals in the amblyopic eye are attenuated in binocular combination, and the fellow eye exerts stronger contrast gain control on the signal in the amblyopic eye and also on the contrast gain control signal from the amblyopic eye (direct and indirect interocular inhibition).

The present study confirmed our earlier finding on binocular phase combination in anisometropic amblyopia, i.e., the amblyopic eye is significantly weakened in binocular phase combination, and there is no significant correlation between the effective contrast in binocular phase combination and visual acuity in the amblyopic eye (Pearson's $R = -0.63$, $P > 0.35$) nor between the equivalent contrast in binocular phase combination and contrast sensitivity (Pearson's $R = 0.77$, $P > 0.40$; Huang et al., 2009). The finding that increasing the base contrast in the amblyopic eye reduced the effective contrast ratio in binocular phase combination is consistent with previous results (Ding et al., 2009), which suggest contributions from stronger contrast gain control of the fellow eye on the contrast gain control signal from the amblyopic eye.

The finding of a significant effect of the probe eye condition in binocular contrast combination conflicts with many studies reporting normal or near normal suprathreshold contrast perception in anisometropic amblyopia (Hess, Bradley, & Piotrowski, 1983; Loshin & Levi, 1983). One major difference between the present study and those in the literature is our use of concurrent, side-by-side presentation of test and probe gratings, whereas previous studies used sequential presentation. It is possible that the different stimulus layout and timing may have led to different interocular interactions. On the other hand, it is worth noting that the probe eye effect, with an average effective ratio (amblyopic to fellow eye) of 0.74, is relatively small compared to the effect of amblyopia on binocular phase and contrast combination. Moreover, when both the test and probe gratings are presented to the amblyopic eye, contrast matching is essentially veridical (matched contrasts = 0.17 ± 0.02, 0.29 ± 0.04, and 0.60 ± 0.06 (mean $\pm$ *SD*)) in the three base contrast conditions (0.16, 0.32, and 0.64, respectively). This suggests that subjects can reliably judge stimulus contrast in the amblyopic eye.

Consistent with our results on normal subjects, we found that binocular contrast combination is independent of the relative phase of the two monocular test gratings, which suggests that the phase and contrast of the cyclopean percepts were computed in separate pathways. Indeed, the idea of multiple pathways for binocular combination is consistent with physiological findings of simple and complex cells in the primary visual cortex (Hubel & Wiesel, 1962). Whereas simple cells receive geniculate inputs and are phase sensitive, complex cells receive the pooled outputs

of simple cells and are phase invariant (Chance, Nelson, & Abbott, 1999; Hubel & Wiesel, 1962). Therefore, it is possible that binocular phase combination is carried out in simple cells, and the phase-invariant binocular contrast combination is carried out in complex cells or beyond. In fact, amblyopia may affect simple and complex cells in different ways. For example, complex cells exhibited higher levels of non-specific excitation and greater fluctuation in response to the deprived eye (the eye that was deprived of visual stimulation during the critical period of visual development) stimulation than did simple cells, following bicuculline-ejecting currents to restore binocularity following deprivation (Burchfiel & Duffy, 1981).

In this study, we investigated the appearance of the cyclopean images resulting from suprathreshold binocular contrast combination of monocular sine-wave gratings with relative phase shifts up to 135 deg. We did not study larger phase differences, due to binocular rivalry in those conditions. It would be necessary to further test if the MCM can be used to model phenomena in near-threshold conditions because appearance and contrast detection may be computed in separate pathways (Blaser, Sperling, & Lu, 1999). For example, Blakemore and Hague (1972) found that two in-phase sinusoidal gratings in the two eyes were more readily detected than out-of-phase gratings, even though the magnitude of detectability improvement was small. Others have also documented that binocular advantage is higher for the in-phase than the out-of-phase condition in contrast discrimination of suprathreshold gratings (Meese, Georgeson, & Baker, 2006; Simmons, 2005). The phase-dependent effect in binocular detection is reversed and enlarged when gratings were displayed in either narrowband (Henning & Hertz, 1973) or broadband (Henning & Hertz, 1977) visual masking noise. It would also be interesting to investigate binocular combination in external noise (Ding & Sperling, 2006, 2007).

The contrast pathway of the MCM is closely related to the two-stage contrast gain control model proposed by Meese et al. (2006), which was successful in modeling contrast matching and contrast discrimination (Baker, Meese, & Georgeson, 2007). The phase pathway of the MCM is identical to that of Ding and Sperling (2006, 2007). The MCM extends both the Ding–Sperling and Meese et al. models by explicitly considering both the phase and contrast in binocular combination. As shown in Figure 2, data from both phase and contrast combination are necessary to quantify the mechanisms of amblyopia.

A number of psychophysical studies have found low or zero binocular summation ratios at high spatial frequencies in amblyopia (Levi, Harwerth, & Manny, 1979; Pardhan & Gilchrist, 1992). Physiological studies on kittens with artificially induced strabismus (Chino, Smith, Yoshida, Cheng, & Hamamoto, 1994; Hubel & Wiesel, 1965) or anisometropia (Eggers & Blakemore, 1978; Kiorpes, Kiper, O'Keefe, Cavanaugh, & Movshon, 1998) have found a lack of binocularly driven neurons. Several recent studies on strabismic amblyopia concluded that binocular combination in strabismic amblyopia is normal when the contrast in amblyopic eye was normalized by the interocular contrast sensitivity ratio (Baker et al., 2008; Baker, Meese, Mansouri, & Hess, 2007; Mansouri, Thompson, & Hess, 2008). In the present study, we focused on anisometropic amblyopia, which is mechanistically different from strabismic amblyopia (Ciuffreda et al., 1991; Hess et al., 1983; McKee et al., 2003), and used horizontal gratings of a low spatial frequency, to which the contrast sensitivities of the two eyes were comparable. We found that anisometropic amblyopia led to both monocular and binocular deficits.

Most current theories on amblyopia have focused on monocular deficits in the visual pathway associated with the amblyopic eye, such as signal attenuation (Baker et al., 2008), under-sampling (Levi & Klein, 1986), topological jittering (Hess et al., 1999), reduced synchronization (Roelfsema et al., 1994), elevated internal noise (Baker et al., 2008; Huang et al., 2007; Levi & Klein, 2003; Xu et al., 2006), and suboptimal perceptual template (Levi & Klein, 2003; Xu et al., 2006), based on results from "eye-isolated" paradigms that only present stimuli in the amblyopic eye. It would be interesting to perform those experiments with and without stimuli in the fellow eye. Such studies would allow us to elaborate the monocular theories in the literature and greatly improve our understanding of mechanisms of amblyopia.

Our results also have important theoretical and clinical implications. Studies in normal subjects have found that stereoacuity depends on the contrast ratio of the inputs to the two eyes (Halpern & Blake, 1988; Legge & Gu, 1989). Obtaining "true" measures of the stereoacuity of amblyopes, therefore, depends on equating the effective contrasts of the two eyes. The paradigm developed in this article makes it possible to measure and equate the effective contrasts of the two eyes in suprathreshold vision. Following the demonstration of effective monocular perceptual learning treatments on amblyopia (Huang, Zhou, & Lu, 2008; Polat, Ma-Naim, Belkin, & Sagi, 2004; Zhou et al., 2006), several research groups (Ding & Levi, 2010; Li, Polat, Makous, & Bavelier, 2009; Li, Ngo, Nguyen, & Levi, in press; Sale et al., 2007) are actively engaged in developing binocular training programs for amblyopia. A good understanding of both the monocular and binocular deficits in amblyopia is extremely important for the development of any binocular rehabilitation programs.

Appendix A: Multi-pathway contrast gain control model (MCM) of binocular combination for normal subjects

The multi-pathway contrast gain control model (MCM) of binocular combination elaborates the Ding–Sperling binocular combination model (Ding & Sperling, 2006,

2007) in two ways: (1) The perceived phase and contrast of the cyclopean images are computed in separate pathways, although with shared cross-eye contrast gain control; and (2) phase-independent local energy from the two monocular images is used in contrast combination. We briefly describe the MCM in this appendix.

The input signals for binocular combination, the two monocular sine-wave gratings, are defined as

$$\mathrm{Lum_L}(y) = L_0\left[1 - C_0\cos\left(2\pi f y \pm \frac{\theta}{2}\right)\right], \tag{A1}$$

$$\mathrm{Lum_R}(y) = L_0\left[1 - \delta C_0\cos\left(2\pi f y \mp \frac{\theta}{2}\right)\right], \tag{A2}$$

where L_0 is the background luminance, f is the spatial frequency of the gratings, C_0 is the base contrast, and δ is the interocular contrast ratio. The two gratings are phase-shifted in opposite directions by $\frac{\theta}{2}$, with a total phase difference of θ.

The input signals first go through double interocular contrast gain control (Ding & Sperling, 2006, 2007), in which each eye exerts gain control on the other eye's signal in proportion to its own signal contrast energy, and also gain controls over the other eye's gain control. The signals in the left and right eyes become

$$\mathrm{Lum_L'} = \frac{1}{1 + \frac{\varepsilon_R}{1+\varepsilon_L}}\mathrm{Lum_L}, \tag{A3}$$

$$\mathrm{Lum_R'} = \frac{1}{1 + \frac{\varepsilon_L}{1+\varepsilon_R}}\mathrm{Lum_R}, \tag{A4}$$

where ε_L and ε_R are the total contrast energy presented to the two eyes and are modeled as $\varepsilon_L = \rho C_L^{\gamma 1}$ and $\varepsilon_R = \rho C_R^{\gamma 1}$, ρ is the gain control efficiency of the signal sine-wave grating, and γ_1 is the exponent of the non-linear transducer. In the experiment, we set $C_L = C_0$ and $C_R = \delta C_0$. From Equations A3 and A4, we have

$$\mathrm{Lum_L'} = \frac{1 + \rho C_0^{\gamma_1}}{1 + \rho C_0^{\gamma_1} + \rho\delta^{\gamma_1} C_0^{\gamma_1}}\mathrm{Lum_L}, \tag{A5}$$

$$\mathrm{Lum_R'} = \frac{1 + \rho\delta^{\gamma_1} C_0^{\gamma_1}}{1 + \rho C_0^{\gamma_1} + \rho\delta^{\gamma_1} C_0^{\gamma_1}}\mathrm{Lum_R}. \tag{A6}$$

Following Ding and Sperling (2006), the cyclopean image is computed directly from the sum of $\mathrm{Lum_L'}$ and $\mathrm{Lum_R'}$:

$$\mathrm{Lum'} = \mathrm{Lum_L'} + \mathrm{Lum_R'}. \tag{A7}$$

Substituting Equations A1, A2, A5, and A6 into Equation A7, we obtain

$$\begin{aligned}\mathrm{Lum} &= \frac{1 + \rho C_0^{\gamma_1}}{1 + \rho C_0^{\gamma_1} + \rho\delta^{\gamma_1} C_0^{\gamma_1}} L_0\left[1 - C_0\cos\left(2\pi f y \pm \frac{\theta}{2}\right)\right] \\ &+ \frac{1 + \rho\delta^{\gamma_1} C_0^{\gamma_1}}{1 + \rho C_0^{\gamma_1} + \rho\delta^{\gamma_1} C_0^{\gamma_1}} L_0\left[1 - \delta C_0\cos\left(2\pi f y \mp \frac{\theta}{2}\right)\right] \\ &= \left[\frac{2 + \rho C_0^{\gamma_1} + \rho\delta^{\gamma_1} C_0^{\gamma_1}}{1 + \rho C_0^{\gamma_1} + \rho\delta^{\gamma_1} C_0^{\gamma_1}} - \frac{C_0 + \rho C_0^{1+\gamma_1}}{1 + \rho C_0^{\gamma_1} + \rho\delta^{\gamma_1} C_0^{\gamma_1}}\right. \\ &\cdot \cos\left(2\pi f y \pm \frac{\theta}{2}\right) - \frac{\delta C_0 + \rho\delta^{1+\gamma_1} C_0^{1+\gamma_1}}{1 + \rho C_0^{\gamma_1} + \rho\delta^{\gamma_1} C_0^{\gamma_1}} \\ &\left.\cdot \cos\left(2\pi f y \mp \frac{\theta}{2}\right)\right] L_0.\end{aligned} \tag{A8}$$

Two phase shift conditions are used in our experiment. When the phase is $\frac{\theta}{2}$ in the left eye and $-\frac{\theta}{2}$ in the right eye, Equation A8 can be rewritten as

$$\begin{aligned}\mathrm{Lum'} &= \left[\frac{2 + \rho C_0^{\gamma_1} + \rho\delta^{\gamma_1} C_0^{\gamma_1}}{1 + \rho C_0^{\gamma_1} + \rho\delta^{\gamma_1} C_0^{\gamma_1}} - C'_{\mathrm{DS1}}\right. \\ &\left.\times \cos\left(2\pi f y + \theta'_{\mathrm{DS1}}\right)\right] L_0,\end{aligned} \tag{A9}$$

with

$$C_{\mathrm{DS1}} = \sqrt{\left(\frac{C_0 + \rho C_0^{1+\gamma_1}}{1 + \rho C_0^{\gamma_1} + \rho\delta^{\gamma_1} C_0^{\gamma_1}}\right)^2 + \left(\frac{\delta C_0 + \rho\delta^{1+\gamma_1} C_0^{1+\gamma_1}}{1 + \rho C_0^{\gamma_1} + \rho\delta^{\gamma_1} C_0^{\gamma_1}}\right)^2 + 2\frac{(C_0 + \rho C_0^{1+\gamma_1}) \times (\delta C_0 + \rho\delta^{1+\gamma_1} C_0^{1+\gamma_1})}{(1 + \rho C_0^{\gamma_1} + \rho\delta^{\gamma_1} C_0^{\gamma_1})^2}\cos\theta}, \tag{A10}$$

$$\theta'_{\mathrm{DS1}} = \tan^{-1}\left[\frac{1 + \rho C_0^{\gamma_1} - \delta + \rho\delta^{1+\gamma_1} C_0^{\gamma_1}}{1 + \rho C_0^{\gamma_1} - \delta + \rho\delta^{1+\gamma_1} C_0^{\gamma_1}}\tan\left(\frac{\theta}{2}\right)\right]. \tag{A11}$$

Here, we use the subscript "DS" to indicate derivations from the original Ding–Sperling model (Ding & Sperling, 2006, 2007) and thus separate them from the elaborated MCM model.

If the phase is $-\frac{\theta}{2}$ in the left eye and $\frac{\theta}{2}$ in the right eye, Equation A8 can be rewritten as

$$\mathrm{Lum}' = \left[\frac{2+\rho C_0^{\gamma_1}+\rho\delta^{\gamma_1}C_0^{\gamma_1}}{1+\rho C_0^{\gamma_1}+\rho\delta^{\gamma_1}C_0^{\gamma_1}} - C'_{\mathrm{DS2}} \times \cos\left(2\pi f y + \theta'_{\mathrm{DS2}}\right)\right] L_0, \tag{A12}$$

with

$$C_{\mathrm{DS2}} = \sqrt{\left(\frac{C_0+\rho C_0^{1+\gamma_1}}{1+\rho C_0^{\gamma_1}+\rho\delta^{\gamma_1}C_0^{\gamma_1}}\right)^2 + \left(\frac{\delta C_0+\rho\delta^{1+\gamma_1}C_0^{1+\gamma_1}}{1+\rho C_0^{\gamma_1}+\rho\delta^{\gamma_1}C_0^{\gamma_1}}\right)^2 + 2\frac{(C_0+\rho C_0^{1+\gamma_1})\times(\delta C_0+\rho\delta^{1+\gamma_1}C_0^{1+\gamma_1})}{(1+\rho C_0^{\gamma_1}+\rho\delta^{\gamma_1}C_0^{\gamma_1})^2}\cos\theta}, \tag{A13}$$

$$\theta'_{\mathrm{DS2}} = -\tan^{-1}\left[\frac{1+\rho C_0^{\gamma_1}-\delta+\rho\delta^{1+\gamma_1}C_0^{\gamma_1}}{1+\rho C_0^{\gamma_1}-\delta+\rho\delta^{1+\gamma_1}C_0^{\gamma_1}}\tan\left(\frac{\theta}{2}\right)\right]. \tag{A14}$$

To account for possible positional effect, we report the perceived contrast and phase of the cyclopean image as

$$\begin{aligned} C_{\mathrm{DS}} &= \frac{C_{\mathrm{DS1}}+C_{\mathrm{DS2}}}{2} \\ &= \sqrt{\left(\frac{C_0+\rho C_0^{1+\gamma_1}}{1+\rho C_0^{\gamma_1}+\rho\delta^{\gamma_1}C_0^{\gamma_1}}\right)^2 + \left(\frac{\delta C_0+\rho\delta^{1+\gamma_1}C_0^{1+\gamma_1}}{1+\rho C_0^{\gamma_1}+\rho\delta^{\gamma_1}C_0^{\gamma_1}}\right)^2 + 2\frac{(C_0+\rho C_0^{1+\gamma_1})\times(\delta C_0+\rho\delta^{1+\gamma_1}C_0^{1+\gamma_1})}{(1+\rho C_0^{\gamma_1}+\rho\delta^{\gamma_1}C_0^{\gamma_1})^2}\cos\theta}, \end{aligned} \tag{A15}$$

$$\begin{aligned} \theta_{\mathrm{DS}} &= \theta_{\mathrm{DS1}} - \theta_{\mathrm{DS2}} \\ &= 2\tan^{-1}\left[\frac{1+\rho C_0^{\gamma_1}-\delta+\rho\delta^{1+\gamma_1}C_0^{\gamma_1}}{1+\rho C_0^{\gamma_1}-\delta+\rho\delta^{1+\gamma_1}C_0^{\gamma_1}}\tan\left(\frac{\theta}{2}\right)\right]. \end{aligned} \tag{A16}$$

Equation A15 is clearly inconsistent with our observation that the perceived contrast of the cyclopean images is independent of the relative phase of the two monocular sine-wave gratings. When the internal representations of the two monocular gratings are equal, e.g., $\frac{C_0+\rho C_0^{1+\gamma_1}}{1+\rho C_0^{\gamma_1}+\rho\delta^{\gamma_1}C_0^{\gamma_1}} = \frac{\delta C_0+\rho\delta^{1+\gamma_1}C_0^{1+\gamma_1}}{1+\rho C_0^{\gamma_1}+\rho\delta^{\gamma_1}C_0^{\gamma_1}} = C_k$, the Ding–Sperling model will predict a difference of $\sqrt{\frac{2+\sqrt{2}}{2-\sqrt{2}}} \approx 2.41$ for phase shift conditions of 45 and 135 degrees. Instead, a phase-independent computation is required to model our empirical results.

We added an independent contrast pathway to the Ding–Spering binocular combination model. In this pathway, the phase information in $\mathrm{Lum}'_{\mathrm{L}}$ and $\mathrm{Lum}'_{\mathrm{R}}$ is discarded. Following interocular contrast gain control, contrast energies in the two eyes are extracted and combined to predict the perceived contrast of the cyclopean image:

$$C' = \left[\left(\frac{C_0+\rho C_0^{1+\gamma_1}}{1+\rho C_0^{\gamma_1}+\rho\delta^{\gamma_1}C_0^{\gamma_1}}\right)^{\gamma_2} + \left(\frac{\delta C_0+\rho\delta^{1+\gamma_1}C_0^{1+\gamma_1}}{1+\rho C_0^{\gamma_1}+\rho\delta^{\gamma_1}C_0^{\gamma_1}}\right)^{\gamma_2}\right]^{1/\gamma_2}. \tag{A17}$$

The computation in the phase pathway is the same as that of the original Ding–Sperling model. The perceived phase difference between the two experimental configurations is

$$\theta' = 2\tan^{-1}\left[\frac{1+\rho C_0^{\gamma_1}-\delta+\rho\delta^{1+\gamma_1}C_0^{\gamma_1}}{1+\rho C_0^{\gamma_1}-\delta+\rho\delta^{1+\gamma_1}C_0^{\gamma_1}}\tan\left(\frac{\theta}{2}\right)\right]. \tag{A18}$$

Together, three free parameters, ρ, γ_1, and γ_2, are used to model the perceived phase and contrast of the cyclopean image in binocular combination.

Appendix B: Multi-pathway contrast gain control model of binocular combination for amblyopia

We considered three possible mechanisms of amblyopia within the framework of the MCM (Figure 2): signal attenuation in the amblyopic eye (A1), stronger contrast gain control of the fellow eye on the amblyopic eye (direct interocular inhibition; A2), and stronger effects on the gain control signal from the amblyopic eye (indirect interocular inhibition; A3). All these mechanisms are modeled as modulators on the corresponding pathways in the MCM.

Following similar derivations in Appendix A, if all three mechanisms are invoked, the perceived phase of the cyclopean image is defined by

$$\theta' = 2\tan^{-1}\left[\frac{\frac{A_1C_0+\rho A_1^{1+\gamma_1}C_0^{1+\gamma_1}}{1+\rho A_1^{\gamma_1}C_0^{\gamma_1}+A_2\rho\delta^{\gamma_1}C_0^{\gamma_1}}-\frac{\delta C_0+A_3\rho\delta^{1+\gamma_1}C_0^{1+\gamma_1}}{1+\rho A_1^{\gamma_1}C_0^{\gamma_1}+A_3\rho\delta^{\gamma_1}C_0^{\gamma_1}}}{\frac{A_1C_0+\rho A_1^{1+\gamma_1}C_0^{1+\gamma_1}}{1+\rho A_1^{\gamma_1}C_0^{\gamma_1}+A_2\rho\delta^{\gamma_1}C_0^{\gamma_1}}+\frac{\delta C_0+A_3\rho\delta^{1+\gamma_1}C_0^{1+\gamma_1}}{1+\rho A_1^{\gamma_1}C_0^{\gamma_1}+A_3\rho\delta^{\gamma_1}C_0^{\gamma_1}}}\tan\left(\frac{\theta}{2}\right)\right], \quad \text{(B1)}$$

$$C' = \left[\left(\frac{A_1C_0+\rho A_1^{1+\gamma_1}C_0^{1+\gamma_1}}{1+\rho A_1^{\gamma_1}C_0^{\gamma_1}+A_2\rho\delta^{\gamma_1}C_0^{\gamma_1}}\right)^{\gamma_2}+\left(\frac{\delta C_0+A_3\rho\delta^{1+\gamma_1}C_0^{1+\gamma_1}}{1+\rho A_1^{\gamma_1}C_0^{\gamma_1}+A_3\rho\delta^{\gamma_1}C_0^{\gamma_1}}\right)^{\gamma_2}\right]^{1/\gamma_2}. \quad \text{(B2)}$$

If A2 is equal to A3, the equations can be simplified as

$$\theta' = 2\tan^{-1}\left[\frac{A_1+\rho A_1^{1+\gamma_1}C_0^{\gamma_1}-\delta-A_2\rho\delta^{1+\gamma_1}C_0^{\gamma_1}}{A_1+\rho A_1^{1+\gamma_1}C_0^{\gamma_1}+\delta+A_2\rho\delta^{1+\gamma_1}C_0^{\gamma_1}}\tan\left(\frac{\theta}{2}\right)\right], \quad \text{(B3)}$$

$$C' = \frac{\left[(A_1C_0+\rho A_1^{1+\gamma_1}C_0^{1+\gamma_1})^{\gamma_2}+(\delta C_0+A_2\rho\delta^{1+\gamma_1}C_0^{1+\gamma_1})^{\gamma_2}\right]^{1/\gamma_2}}{1+\rho A_1^{\gamma_1}C_0^{\gamma_1}+A_2\rho\delta^{\gamma_1}C_0^{\gamma_1}}. \quad \text{(B4)}$$

When the two eyes contribute equally in binocular phase combination, i.e., $\theta' = 0$, we obtain the following from Equation B3:

$$A_1+\rho A_1^{1+\gamma_1}C_0^{\gamma_1} = \delta + A_2\rho\delta^{1+\gamma_1}C_0^{\gamma_1}. \quad \text{(B5)}$$

Substituting Equation B5 into Equation B4, when $\theta' = 0$, we have

$$C' = \frac{2^{1/\gamma_2}A_1C_0(1+\rho A_1^{\gamma_1}C_0^{\gamma_1})}{1+\rho A_1^{\gamma_1}C_0^{\gamma_1}+A_2\rho\delta^{\gamma_1}C_0^{\gamma_1}}. \quad \text{(B6)}$$

If $\rho \gg 1$ and C_0 is large, we can ignore those terms that do not include ρ in Equations B5 and B6 and obtain the following approximations:

$$\delta = \frac{A_1}{A_2^{1/(1+\gamma_1)}}, \quad \text{(B7)}$$

$$C' = \frac{2^{1/\gamma_2}A_1^{1+\gamma_1}}{A_1^{\gamma_1}+A_2\delta^{\gamma_1}}C_0. \quad \text{(B8)}$$

Equations B7 and B8 shows that the effective contrast ratio of the amblyopic eye in phase combination and the perceived contrast of the cyclopean grating when $\theta' = 0$ are determined by three factors, A_1, A_2, and γ_1. If we assume that γ_1 is normal and can be obtained from the literature (Huang et al., 2010), the two equations allow us to solve for A_1 and A_2. Therefore, the minimum experiment that is required to determine A_1 and A_2 should consist of measurements of the effective contrast ratio of the amblyopic eye (when $\theta' = 0$) in phase combination and the corresponding perceived contrast of the cyclopean image. These equations also provide some intuitions as to why phase measurement was not sufficient to distinguish mechanisms of amblyopia; a single equation (Equation B7) is not sufficient to specify both A_1 and A_2.

Acknowledgments

The National Eye Institute (EY017491) and the National Natural Science Foundation of China (30630027) supported the research. We thank Dr. Luis Lesmes for valuable comments on the manuscript.

Author's contribution: Chang-Bing Huang and Jiawei Zhou contributed equally to this work.
Commercial relationships: none.
Corresponding author: Zhong-Lin Lu.
Email: zhonglin@usc.edu.
Address: Laboratory of Brain Processes (LOBES), Department of Psychology, University of Southern California, Los Angeles, CA 90089, USA.

References

Baker, D. H., Meese, T. S., & Georgeson, M. A. (2007). Binocular interaction: Contrast matching and contrast discrimination are predicted by the same model. *Spatial Vision, 20,* 397–413. [PubMed]

Baker, D. H., Meese, T. S., & Hess, R. F. (2008). Contrast masking in strabismic amblyopia: Attenuation, noise, interocular suppression and binocular summation. *Vision Research, 48,* 1625–1640. [PubMed]

Baker, D. H., Meese, T. S., Mansouri, B., & Hess, R. F. (2007). Binocular summation of contrast remains intact in strabismic amblyopia. *Investigative Ophthalmology and Visual Science, 48,* 5332–5338. [PubMed]

Blakemore, C., & Hague, B. (1972). Evidence for disparity detecting neurones in the human visual system. *The Journal of Physiology, 225,* 437–455. [PubMed] [Article]

Blaser, E., Sperling, G., & Lu, Z. L. (1999). Measuring the amplification of attention. *Proceedings of the National Academy of Sciences of the United States of America, 96,* 11681–11686. [PubMed] [Article]

Bonneh, Y. S., Sagi, D., & Polat, U. (2007). Spatial and temporal crowding in amblyopia. *Vision Research, 47,* 1950–1962. [PubMed]

Bradley, A., & Freeman, R. D. (1981). Contrast sensitivity in anisometropic amblyopia. *Investigative Ophthalmology and Visual Science, 21,* 467–476. [PubMed]

Brainard, D. H. (1997). The psychophysics toolbox. *Spatial Vision, 10,* 433–436. [PubMed]

Burchfiel, J. L., & Duffy, F. H. (1981). Role of intracortical inhibition in deprivation amblyopia: Reversal by microiontophoretic bicuculline. *Brain Research, 206,* 479–484. [PubMed]

Chance, F. S., Nelson, S. B., & Abbott, L. F. (1999). Complex cells as cortically amplified simple cells. *Nature Neuroscience, 2,* 277–282. [PubMed]

Chino, Y. M., Smith, E. L., 3rd, Yoshida, K., Cheng, H., & Hamamoto, J. (1994). Binocular interactions in striate cortical neurons of cats reared with discordant visual inputs. *Journal of Neuroscience, 14,* 5050–5067. [PubMed] [Article]

Ciuffreda, K. J., Levi, D. M., & Selenow, A. (1991). *Amblyopia: Basic and clinical aspects*. Boston: Butterworth-Heinemann.

Cormack, L. K., Stevenson, S. B., & Landers, D. D. (1997). Interactions of spatial frequency and unequal monocular contrasts in stereopsis. *Perception, 26,* 1121–1136. [PubMed]

Ding, J., Klein, S., & Levi, D. (2009). Binocular combination in amblyopic vision [Abstract]. *Journal of Vision, 9*(8):274, 274a, http://www.journalofvision.org/content/9/8/274, doi:10.1167/9.8.274.

Ding, J., & Levi, D. (2010). Recovery of stereopsis in human adults with strabismus through perceptual learning [Abstract]. *Journal of Vision, 10*(7):1124, 1124a, http://www.journalofvision.org/content/10/7/1124, doi:10.1167/10.7.1124.

Ding, J., & Sperling, G. (2006). A gain-control theory of binocular combination. *Proceedings of the National Academy of Sciences of the United States of America, 103,* 1141–1146. [PubMed] [Article]

Ding, J., & Sperling, G. (2007). Binocular combination: Measurements and a model. In L. Harris & M. Jenkin (Eds.), *Computational vision in neural and machine systems* (pp. 257–305). Cambridge, UK: Cambridge University Press.

Dudley, L. P. (1951). *Stereoptics: An introduction*. London: MacDonald & Co.

Eggers, H. M., & Blakemore, C. (1978). Physiological basis of anisometropic amblyopia. *Science, 201,* 264–267. [PubMed]

Halpern, D. L., & Blake, R. R. (1988). How contrast affects stereoacuity. *Perception, 17,* 483–495. [PubMed]

Harrad, R. A., & Hess, R. F. (1992). Binocular integration of contrast information in amblyopia. *Vision Research, 32,* 2135–2150. [PubMed]

Harwerth, R. S., & Levi, D. M. (1983). Psychophysical studies on the binocular processes of amblyopes. *American Journal of Optometry and Physiological Optics, 60,* 454–463. [PubMed]

Henning, G. B., & Hertz, B. G. (1973). Binocular masking level differences in sinusoidal grating detection. *Vision Research, 13,* 2455–2463. [PubMed]

Henning, G. B., & Hertz, B. G. (1977). The influence of bandwidth and temporal properties of spatial noise on binocular masking-level differences. *Vision Research, 17,* 399–402. [PubMed]

Hess, R. F., Bradley, A., & Piotrowski, L. (1983). Contrast-coding in amblyopia: I. Differences in the neural basis of human amblyopia. *Proceedings of the Royal Society of London B: Biological Sciences, 217,* 309–330. [PubMed]

Hess, R. F., & Demanins, R. (1998). Contour integration in anisometropic amblyopia. *Vision Research, 38,* 889–894. [PubMed]

Hess, R. F., Thompson, B., Gole, G., & Mullen, K. T. (2009). Deficient responses from the lateral geniculate nucleus in humans with amblyopia. *European*

Journal of Neuroscience, 29, 1064–1070. [PubMed] [Article]

Hess, R. F., Wang, Y. Z., Demanins, R., Wilkinson, F., & Wilson, H. R. (1999). A deficit in strabismic amblyopia for global shape detection. *Vision Research, 39,* 901–914. [PubMed]

Huang, C. B., Tao, L., Zhou, Y., & Lu, Z. L. (2007). Treated amblyopes remain deficient in spatial vision: A contrast sensitivity and external noise study. *Vision Research, 47,* 22–34. [PubMed]

Huang, C. B., Zhou, Y., & Lu, Z. L. (2008). Broad bandwidth of perceptual learning in the visual system of adults with anisometropic amblyopia. *Proceedings of the National Academy Sciences of the United States of America, 105,* 4068–4073. [PubMed] [Article]

Huang, C. B., Zhou, J., Lu, Z. L., Feng, L., & Zhou, Y. (2009). Binocular combination in anisometropic amblyopia. *Journal of Vision, 9*(3):17, 1–16, http://www.journalofvision.org/content/9/3/17, doi:10.1167/9.3.17. [PubMed] [Article]

Huang, C. B., Zhou, J., Zhou, Y., & Lu, Z. L. (2010). Contrast and phase combination in binocular vision. *PLoS One, 5,* e15075. [PubMed] [Article]

Hubel, D. H., & Wiesel, T. N. (1962). Receptive fields, binocular interaction and functional architecture in the cat's visual cortex. *The Journal of Physiology, 160,* 106–154. [PubMed] [Article]

Hubel, D. H., & Wiesel, T. N. (1965). Binocular interaction in striate cortex of kittens reared with artificial squint. *Journal of Neurophysiology, 28,* 1041–1059. [PubMed] [Article]

Kiorpes, L., Kiper, D. C., O'Keefe, L. P., Cavanaugh, J. R., & Movshon, J. A. (1998). Neuronal correlates of amblyopia in the visual cortex of macaque monkeys with experimental strabismus and anisometropia. *Journal of Neuroscience, 18,* 6411–6424. [PubMed] [Article]

Kiorpes, L., & McKee, S. P. (1999). Neural mechanisms underlying amblyopia. *Current Opinion on Neurobiology, 9,* 480–486. [PubMed]

Legge, G. E., & Gu, Y. C. (1989). Stereopsis and contrast. *Vision Research, 29,* 989–1004. [PubMed]

Levi, D. M., Harwerth, R. S., & Manny, R. E. (1979). Suprathreshold spatial frequency detection and binocular interaction in strabismic and anisometropic amblyopia. *Investigative Ophthalmology and Visual Science, 18,* 714–725. [PubMed]

Levi, D. M., & Klein, S. A. (1986). Sampling in spatial vision. *Nature, 320,* 360–362. [PubMed]

Levi, D. M., & Klein, S. A. (2003). Noise provides some new signals about the spatial vision of amblyopes. *Journal of Neuroscience, 23,* 2522–2526. [PubMed] [Article]

Li, R., Polat, U., Makous, W., & Bavelier, D. (2009). Enhancing the contrast sensitivity function through action video game training. *Nature Neuroscience, 12,* 549–551. [PubMed]

Li, R. W., Ngo, C., Nguyen, J., & Levi, D. (in press). Video game play induces plasticity in the visual system of adults with amblyopia. *PLoS Biology*.

Li, X., Lu, Z. L., Xu, P., Jin, J., & Zhou, Y. (2003). Generating high gray-level resolution monochrome displays with conventional computer graphics cards and color monitors. *Journal of Neuroscience Methods, 130,* 9–18. [PubMed]

Loshin, D. S., & Levi, D. M. (1983). Suprathreshold contrast perception in functional amblyopia. *Documenta Ophthalmologica, 55,* 213–236. [PubMed]

Mansouri, B., Thompson, B., & Hess, R. F. (2008). Measurement of suprathreshold binocular interactions in amblyopia. *Vision Research, 48,* 2775–2784. [PubMed]

McKee, S. P., Levi, D. M., & Movshon, J. A. (2003). The pattern of visual deficits in amblyopia. *Journal of Vision, 3*(5):5, 380–405, http://www.journalofvision.org/content/3/5/5, doi:10.1167/3.5.5. [PubMed] [Article]

Meese, T. S., Georgeson, M. A., & Baker, D. H. (2006). Binocular contrast vision at and above threshold. *Journal of Vision, 6*(11):7, 1224–1243, http://www.journalofvision.org/content/6/11/7, doi:10.1167/6.11.7. [PubMed] [Article]

Mitchell, D. E., Kind, P. C., Sengpiel, F., & Murphy, K. (2003). Brief daily periods of binocular vision prevent deprivation-induced acuity loss. *Current Biology, 13,* 1704–1708. [PubMed]

Mitchell, D. E., Reardon, J., & Muir, D. W. (1975). Interocular transfer of the motion after-effect in normal and stereoblind observers. *Experimental Brain Research, 22,* 163–173. [PubMed]

Pardhan, S., & Gilchrist, J. (1992). Binocular contrast summation and inhibition in amblyopia. The influence of the interocular difference on binocular contrast sensitivity. *Documenta Ophthalmologica, 82,* 239–248. [PubMed]

Pelli, D. G. (1997). The VideoToolbox software for visual psychophysics: Transforming numbers into movies. *Spatial Vision, 10,* 437–442. [PubMed]

Polat, U., Ma-Naim, T., Belkin, M., & Sagi, D. (2004). Improving vision in adult amblyopia by perceptual learning. *Proceedings of the National Academy of*

Sciences of the United States of America, 101, 6692–6697. [PubMed] [Article]

Pugh, M. (1954). Foveal vision in amblyopia. *British Journal of Ophthalmology, 38,* 321–331. [PubMed]

Roelfsema, P. R., Konig, P., Engel, A. K., Sireteanu, R., & Singer, W. (1994). Reduced synchronization in the visual cortex of cats with strabismic amblyopia. *European Journal of Neuroscience, 6,* 1645–1655. [PubMed]

Sale, A., Maya Vetencourt, J. F., Medini, P., Cenni, M. C., Baroncelli, L., De Pasquale, R., et al. (2007). Environmental enrichment in adulthood promotes amblyopia recovery through a reduction of intracortical inhibition. *Nature Neuroscience, 10,* 679–681. [PubMed]

Sharma, V., Levi, D. M., & Klein, S. A. (2000). Undercounting features and missing features: Evidence for a high-level deficit in strabismic amblyopia. *Nature Neuroscience, 3,* 496–501. [PubMed]

Simmers, A. J., Ledgeway, T., Hess, R. F., & McGraw, P. V. (2003). Deficits to global motion processing in human amblyopia. *Vision Research, 43,* 729–738. [PubMed]

Simmons, D. R. (2005). The binocular combination of chromatic contrast. *Perception, 34,* 1035–1042. [PubMed]

Smith, S. L., & Trachtenberg, J. T. (2007). Experience-dependent binocular competition in the visual cortex begins at eye opening. *Nature Neuroscience, 10,* 370–375. [PubMed]

Wheatstone, C. (1838). Contributions to the physiology of vision—Part the first. On some remarkable, and hitherto unobserved, phenomena of binocular vision. *Philosophical Transactions of the Royal Society, 128,* 371–394.

Wood, I. C., Fox, J. A., & Stephenson, M. G. (1978). Contrast threshold of random dot stereograms in anisometropic amblyopia: A clinical investigation. *British Journal of Ophthalmology, 62,* 34–38. [PubMed]

Xu, P., Lu, Z. L., Qiu, Z., & Zhou, Y. (2006). Identify mechanisms of amblyopia in Gabor orientation identification with external noise. *Vision Research, 46,* 3748–3760. [PubMed]

Zhou, Y., Huang, C., Xu, P., Tao, L., Qiu, Z., Li, X., et al. (2006). Perceptual learning improves contrast sensitivity and visual acuity in adults with anisometropic amblyopia. *Vision Research, 46,* 739–750. [PubMed]